

Analysis and Evaluation of Bi-Directional Power Switch Losses for Matrix Converter Drive

Jun-Koo Kang, Hidenori Hara, Eiji Yamamoto, Eiji Watanabe

Yaskawa Electric Corporation
12-1 Ohtemachi, Kokura-Kita-Ku, Kitakyushu-City, 803-8530, Japan
e-mail : kang@yaskawa.co.jp

Abstract — The matrix converter (MC) is a bi-directional ac/ac conversion device that generates variable-voltage variable-frequency output from ac voltage utility. Since power topology and switching rules of MC are quite different from voltage source inverter (VSI), power device loss analysis based on VSI topology cannot be applied to MC. In this paper, analysis method for evaluation of bi-directional switch losses of MC is proposed. Variation of collector-emitter voltage and current distribution in bi-directional IGBTs are investigated at various operating conditions for power loss analysis. The validity of the proposed analysis has been verified through the simulations and the experimental results with 7.5 kW MC driven-ac drives system.

Keywords—Bi-directional switch; conduction loss; IGBT; matrix converter; power loss; reverse recovery; switching loss

I. INTRODUCTION

The matrix converter (MC) is an ac-to-ac bi-directional power conversion topology that generates variable-voltage variable-frequency output from ac voltage utility with no intermediate dc link [1-3]. MC has high power quality, i.e. sinusoidal currents with unity power factor, and it is fully regenerative. Due to the increasing importance of power quality and energy efficiency in power electronics industries, the progress of MC technology has been further accelerated. Fig.1 shows the basic MC drive structure that consists of nine 9 bi-directional switches. To bring MC concept to a commercial product, low-power loss and compact bi-directional IGBT switches are the essential hardware elements. Owing to the rapid progress of power device technologies, a special purpose IGBT module for MC is reported by a power semiconductor manufacturer [4], and bi-directional IGBTs that have reverse blocking capability are also reported [5].

Power loss analysis on bi-directional switches is one of basic steps for evaluation of the reliability of MC. Since power topologies and switching rules of MC are quite different from voltage source inverter (VSI), loss analysis methods used for power switches of VSI topology cannot be applied to MC. In MC system, ac utility voltages are directly converted into variable voltage outputs using nine bi-directional switches with no dc-link voltage and no associated large capacitors. As a result, the collector-emitter voltage

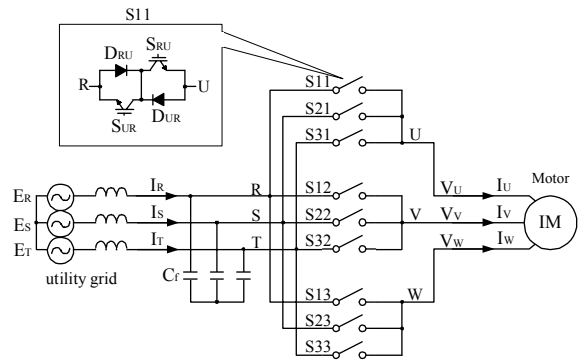


Fig. 1. The basic structure of a matrix converter drive.

V_{ce} of IGBT modules are not constant at each switching instant, and current distribution in each power device changes because of the rotation of voltage angle of utility grid even if output current is constant. For this reason, evaluation of switching losses in MC requires conceptual understanding of switching rules and physical characteristics of IGBTs and diodes. There have been a lot of researches on MC. But detailed loss analysis of bi-directional switches according to switching rules has not been presented yet.

This paper presents an analysis method for evaluating power device losses of MC that consist of switching and conduction losses of IGBTs and diodes. Since the total switching loss is dependent on the modulation scheme, switching rules of MC are explained briefly, and then variations of collector-emitter voltage and current distribution in bi-directional switches are investigated. Mathematical descriptions of the power dissipation of IGBTs and diodes are presented based on the investigation. To verify the validity of the proposed analysis, mathematical analysis results are compared with experimental results. For experiments, 600V, 75A bi-directional switch modules for MC are developed by integrating power IGBTs and diodes into one package.

II. CONTROL PRINCIPLE OF MATRIX CONVERTER

A. PWM Switching Rule

The PWM modulation strategy reported in [6,7] has been employed in this paper because of good input current control characteristics even under unbalanced input voltage conditions.

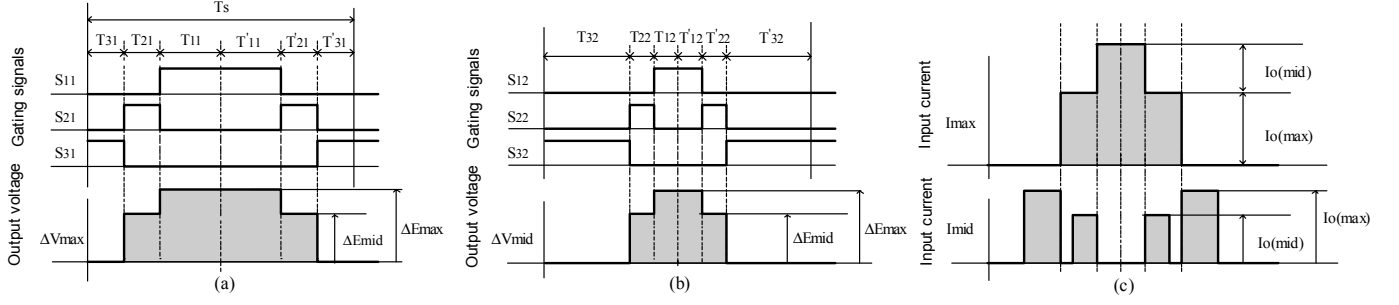


Fig.2. PWM switching pattern and line-to-line output voltages:
(a) Vmax ; (b) Vmid ; (c) two input currents.

The PWM pattern, line-to-line output voltages, and input currents are shown in Fig. 2. In the figure above, switches S_{13} and S_{23} remain in the off-state, and S_{33} remains in the on-state while other switches are PWM controlled over the carrier period T_s . Input phase voltages E_R , E_S , and E_T are sorted and labeled as E_{\max} , E_{mid} , and E_{\min} respectively according to their value. The base voltage E_{base} is defined as the input phase voltage that has the highest absolute value. The output voltage references $V_{U\text{ref}}$, $V_{V\text{ref}}$ and $V_{W\text{ref}}$ are also sorted and labeled as V_{\max} , V_{mid} and V_{\min} . The some voltage variables are defined as (1)-(4). To concentrate on the loss analysis of bi-directional IGBT, detailed switching rules are not presented in this paper. The details of the sorting rules are described in [6,7].

$$\Delta E_{\max} = E_{\max} - E_{\min} \quad (1)$$

$$\Delta E_{\text{mid}} = \begin{cases} E_{\max} - E_{\text{mid}} & \text{if } E_{\text{base}} = E_{\max} \\ E_{\text{mid}} - E_{\min} & \text{if } E_{\text{base}} = E_{\min} \end{cases} \quad (2)$$

$$\Delta V_{\max} = V_{\max} - V_{\min} \quad (3)$$

$$\Delta V_{\text{mid}} = \begin{cases} V_{\max} - V_{\text{mid}} & \text{if } E_{\text{base}} = E_{\max} \\ V_{\text{mid}} - V_{\min} & \text{if } E_{\text{base}} = E_{\min} \end{cases} \quad (4)$$

III. POWER LOSS ANALYSIS OF MATRIX CONVERTER

A. IGBT Conduction Loss (P_{cond})

Average conduction loss of an IGBT device can be expressed as

$$P_{\text{cond}} = \frac{1}{T} \int_0^T V_{CE} \cdot I_C \cdot dt \quad (5)$$

where V_{CE} is collector-emitter voltage, I_C is collector current,

and T is a time period of one output cycle. Generally the I-V characteristic of IGBT can be modeled with a threshold voltage V_{CE0} and an equivalent on-resistance R_k .

$$V_{CE} = V_{CE0} + R_k \cdot I_C \quad (6)$$

Suppose that output current of MC is sinusoidal. Then U-phase current I_u can be defined as $I_u = \sqrt{2}I_o \sin \omega t$ where I_o is rms output current. According to the PWM switching rule in Fig.3, I_{tu} , I_{su} , and I_{ru} flow in turn to U-phase output terminal during one PWM cycle. Average conduction loss of IGBT device that is connected between R-U is

$$\begin{aligned} P_{\text{cond-RU}} &= \frac{1}{T} \int_0^T \frac{t_\gamma}{T_s} \cdot V_{CE} \cdot I_C \cdot dt \\ &= \frac{\sqrt{2}I_o}{T} \int_0^T \frac{t_\gamma}{T_s} (V_{CE0} \sin \omega t + \sqrt{2}R_k I_o \sin^2 \omega t) dt \end{aligned} \quad (7)$$

In the same way,

$$P_{\text{cond-SU}} = \frac{\sqrt{2}I_o}{T} \int_0^T \frac{t_\beta}{T_s} (V_{CE0} \sin \omega t + \sqrt{2}R_k I_o \sin^2 \omega t) dt \quad (8)$$

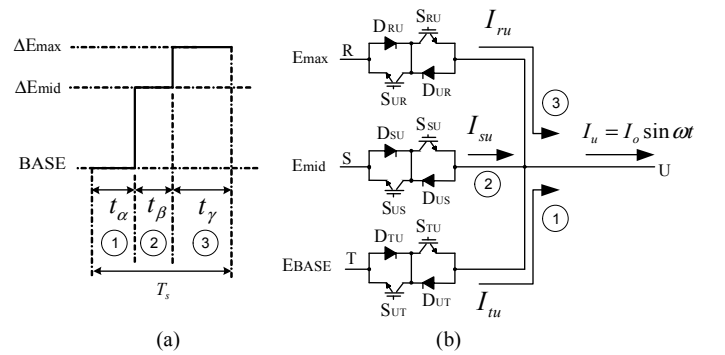


Fig.3. Output voltage and current of MC based on PWM switching rule.

(a) Line to line output voltage based on PWM pattern.

(b) Current distribution in U-phase.

$$P_{cond-TU} = \frac{\sqrt{2}I_o}{T} \int_0^T \frac{t}{T_s} (V_{CE0} \sin \omega t + \sqrt{2}R_k I_o \sin^2 \omega t) dt \quad (9)$$

Thus average conduction loss per phase P_{cond} can be obtained using (7)-(9) as follows

$$P_{cond} = P_{cond-RU} + P_{cond-SU} + P_{cond-TU} = \frac{2\sqrt{2}}{\pi} V_{CE0} I_o + I_o^2 R_k \quad (10)$$

Unlike conventional VSI topology, conduction loss is not concentrated on one switch even if output frequency of MC is very low. It will be discussed later.

B. Diode Conduction Loss (P_{condD})

As can be seen from Fig.3(b), collector currents of IGBTs flow into series connected diodes. Thus diode current I_D is same as I_C , and average conduction loss of diode P_{condD} can be calculated from a similar procedure:

$$P_{condD} = \frac{1}{T} \int_0^T V_{AK} \cdot I_C \cdot dt \quad (11)$$

Anode-cathode voltage V_{AK} in (11) can be modeled as

$$V_{AK} = V_{D0} + R_{Dk} \cdot I_C \quad (12)$$

where V_{D0} is a threshold voltage and R_{Dk} is an equivalent on-resistance. Resulting average diode conduction loss per phase can be obtained as

$$P_{condD} = \frac{2\sqrt{2}}{\pi} V_{D0} I_o + I_o^2 R_{Dk} \quad (13)$$

C. IGBT Turn-on Loss (P_{SWON})

Fig.4 illustrates the generation of power losses of IGBT during one PWM cycle. Suppose that input voltages E_R , E_S , and E_T are sorted into E_{max} , E_{mid} , and E_{min} respectively

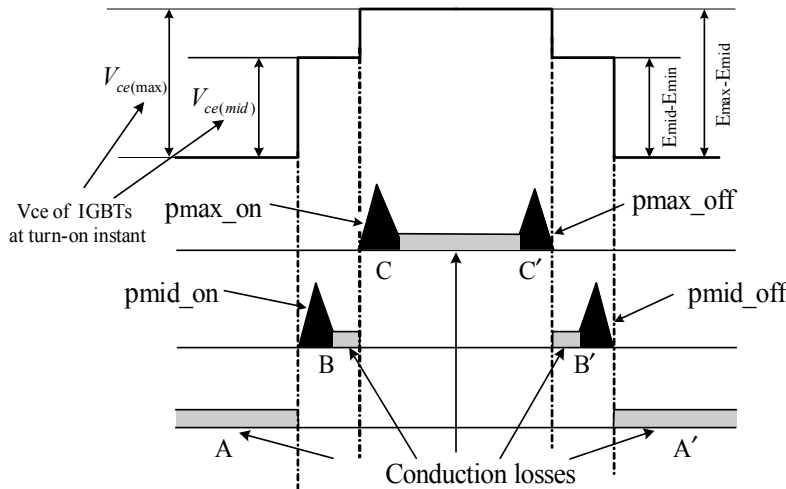


Fig.4. Generation of turn-on and turn-off losses in matrix converter

according to their value. According to switching rules shown in Fig.2, U-phase output is connected to input-phase voltages in the sequence of T, S, and R-phase during one PWM cycle. If output current is positive, IGBTs S_{TU} , S_{SU} , and S_{RU} are conducted sequentially. The turn-on loss of IGBTs per output phase P_{SWON} is sum of two losses p_{mid_ON} and p_{max_ON} that occur at transition instant from A to B, and from B to C respectively.

$$P_{SWON} = p_{mid_ON} + p_{max_ON} \\ = \xi_{tON} V_{ce(mid)} \cdot I_c + \xi_{tON} V_{ce(max)} \cdot I_c \quad (14)$$

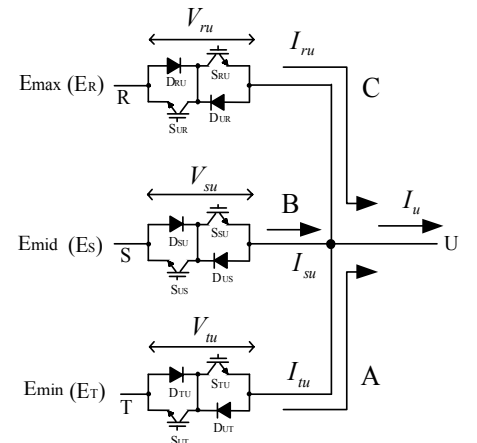
where $V_{ce(mid)}$ and $V_{ce(max)}$ are collector-emitter voltage at the instant of switch transition from A to B, and B to C respectively, and ξ_{tON} is turn-on loss coefficient determined by IGBT characteristics and gate drive resistor. From Fig.4 and (14), average turn-on loss P_{SWON} can be obtained as

$$P_{SWON} = \frac{1}{T} \int_0^T \xi_{tON} (E_{mid} - E_{min}) \cdot I_o \cdot f_c \cdot dt \\ + \frac{1}{T} \int_0^T \xi_{tON} (E_{max} - E_{mid}) \cdot I_o \cdot f_c \cdot dt \\ = \frac{1}{T} \int_0^T \xi_{tON} \Delta E_{max} \cdot I_o \cdot f_c \cdot dt = \xi_{tON} \Delta E_{max_AV} \cdot I_{o_AV} \cdot f_c \quad (15)$$

where ΔE_{max_AV} and I_{o_AV} are averages of maximum line-to-line voltage and output current respectively, and f_c is the carrier frequency. MC system is assumed to have sinusoidal voltage source and output currents then

$$\Delta E_{max_AV} = \frac{6}{\pi} \int_0^{\pi/6} \sqrt{2} V_i \cos \theta \cdot d\theta = \frac{3\sqrt{2}}{\pi} V_i \quad (16)$$

$$I_{o_AV} = \frac{1}{\pi} \int_0^{\pi} \sqrt{2} I_o \sin \theta \cdot d\theta = \frac{2\sqrt{2}}{\pi} I_o \quad (17)$$



where V_i is the rms value of input voltage.

From (15)-(17), resulting average turn-on loss is

$$P_{SWON} = \xi_{ION} \frac{12}{\pi^2} V_i \cdot I_o \cdot f_c \quad (18)$$

D. IGBT Turn-off Loss (P_{SWOFF})

It should be noted in Fig.4 that IGBT turn-off losses are zero at transition instants from A to B, and B to C thanks to the intrinsic zero current switching characteristics. Fig.5 illustrates switch commutation method for transition from A to B shown in Fig.4. When IGBT S_{SU} is turned on, S_{TU} is naturally commutated because reverse voltage $E_{mid} - E_{min}$ is applied to S_{TU} , so conducting device changes from IGBT S_{TU} to S_{SU} . Thus S_{TU} has zero turn-off loss characteristics. Same phenomenon occurs when conducting device changes from S_{SU} to S_{RU} . Therefore turn-off loss can be obtained by only considering transition from C' to B' , and B' to A' . Following a procedure similar to turn-on loss calculation, average turn-on loss P_{SWOFF} can be obtained as

$$\begin{aligned} P_{SWOFF} &= \frac{1}{T} \int_0^T \xi_{IOFF} (E_{max} - E_{mid}) \cdot I_o \cdot f_c \cdot dt \\ &+ \frac{1}{T} \int_0^T \xi_{IOFF} (E_{mid} - E_{min}) \cdot I_o \cdot f_c \cdot dt \\ &= \frac{1}{T} \int_0^T \xi_{IOFF} \Delta E_{max} \cdot I_o \cdot f_c \cdot dt \\ &= \xi_{IOFF} \Delta E_{max_AV} \cdot I_o \cdot f_c \end{aligned} \quad (19)$$

where ξ_{IOFF} is turn-off loss coefficient determined by of IGBT characteristics and gate drive resistor. By substituting (16) and (17) into (19), resulting P_{SWOFF} is obtained as

$$P_{SWOFF} = \xi_{IOFF} \frac{12}{\pi^2} V_i \cdot I_o \cdot f_c \quad (20)$$

E. Diode Reverse Recovery Loss (P_{SWRR})

The turn-on losses of the diode can be neglected in diode switching losses because they are very small. The turn-off recovery losses of diode can be explained from turn-on sequence of IGBT in Fig.4. The reverse recovery losses occur

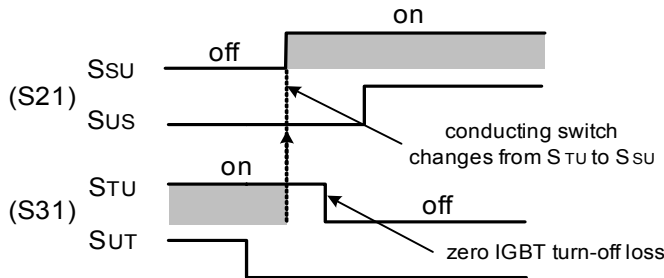


Fig.5. Switch commutation and IGBT turn-off losses in matrix converter

at the instant of switch transition from A to B, and from B to C respectively. Suppose that current flows through D_{SU} and S_{SU} during interval B. During transition from B to C, output current I_u starts to flow through D_{RU} and S_{RU} , and diode recovery loss occurs at D_{SU} as shown in Fig. 6. Average turn-off loss of diode P_{SWRR} can be obtained as

$$\begin{aligned} P_{SWRR} &= \frac{1}{T} \int_0^T \xi_{RR} (E_{max} - E_{mid}) \cdot I_o \cdot f_c \cdot dt \\ &+ \frac{1}{T} \int_0^T \xi_{RR} (E_{mid} - E_{min}) \cdot I_o \cdot f_c \cdot dt \\ &= \frac{1}{T} \int_0^T \xi_{RR} \Delta E_{max} \cdot I_o \cdot f_c \cdot dt \\ &= \xi_{RR} \Delta E_{max_AV} \cdot I_o \cdot f_c \end{aligned} \quad (21)$$

where ξ_{RR} is a reverse recovery loss coefficient determined by of diode characteristics. Resulting P_{SWRR} is obtained as

$$P_{SWRR} = \xi_{RR} \frac{12}{\pi^2} V_i \cdot I_o \cdot f_c \quad (22)$$

IV. COMPARISON BETWEEN LOSS ANALYSIS AND EXPERIMENTS DATA

To verify the validity of the proposed analysis, experimental setup is built using 600V, 75A bi-directional IGBT modules which are developed by integrating IGBTs and diodes into one package. Input voltage is three-phase, 220V, 60Hz. MC system drives three-phase, 200V, 7.5kW vector-controlled induction machine at PWM carrier frequencies of 5kHz, 10kHz, and 15kHz respectively.

A. Total Losses of Matrix Converter

Table I shows simulated and experimented loss analysis results with three kinds of bi-directional IGBT samples that have different electrical characteristics. Experimental measurements show that total losses of each sample range from 212W (2.8% of rated power) to 307W (4.1% of rated power) at 10kHz carrier frequency. Simulation results show

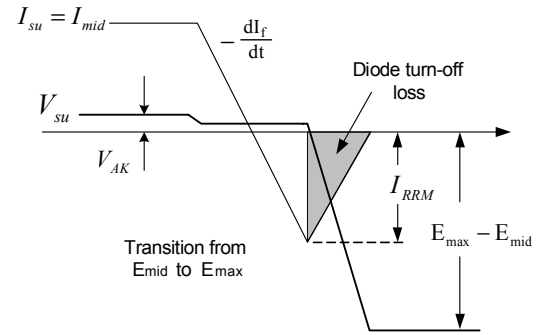


Fig.6. Generation of diode reverse recovery loss in matrix converter

TABLE I. TOTAL LOSS COMPARISON ACCORDING TO CARRIER FREQUENCY OF BI-DIRECTIONAL IGBTs (EXPERIMENTAL RESULT).

Test sample	Carrier frequency	Total Losses at rated power of 7.5 kW		Error [%]
		Simulations [W]	Experiments [W]	
A	5 kHz	205.32	188.93	- 6.07
	10 kHz	221.24	212.23	- 3.07
	15 kHz	238.80	240.83	0.63
B	5 kHz	300.70	300.43	- 0.18
	10 kHz	322.42	307.33	- 3.64
	15 kHz	344.08	331.83	- 2.73
C	5 kHz	269.32	248.23	- 6.41
	10 kHz	282.04	267.93	- 4.05
	15 kHz	297.15	292.43	- 1.26

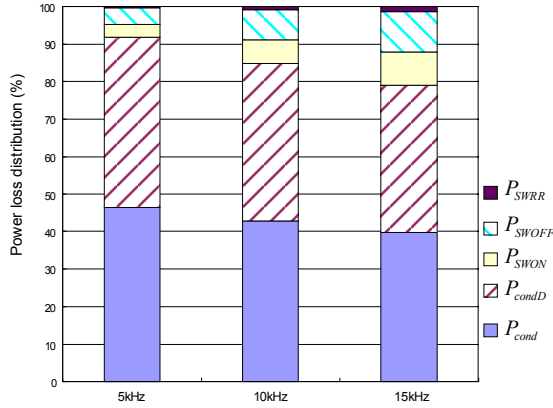


Fig. 7. Simulated IGBT and diode loss distribution in 6in1 package according to carrier frequencies.

reasonably good accuracy with experimental measurements. It must be mentioned that the power loss distribution is determined by many factors including carrier frequency, input voltage, and current levels. Fig. 7 illustrates IGBT and diode loss distribution in 6 in 1 package according to PWM carrier frequency. Total switching losses are in the range of 9 % at 5kHz to 20 % at 15kHz carrier frequency.

B. Current Distribution in Bi-directional IGBT Modules

It is well known that in VSI system, zero frequency output is the most severe operating condition from the viewpoint of inverter cooling because output currents are concentrated on several IGBTs. MC also has current concentration phenomena according to operating condition but it is less severe than VSI. U-phase output current I_u and current I_{ru} that flows into R-U terminal in Fig. 4 are shown to investigate the current distribution in IGBTs according to output frequency.

Figs. 8(a)-(c) shows currents flowing in IGBT under dc output condition. Since U-phase output has one-directional current flow, half of bi-directional IGBTs S_{UR} , S_{US} , and S_{UT} are not used. Thus average current of each IGBT becomes one third

of dc current. Figs. 9(a)-(c) show I_u and I_{ru} at 30Hz output frequency with different phase differences. Since input and output frequencies are not same, phase difference changes continuously. Thus no current concentration occurs, and average current of each IGBT becomes one sixth of average output current. Figs. 10(a)-(c) show I_u and I_{ru} at 60Hz output frequency. It can be seen that I_{ru} has different waveforms with three different phase differences between input voltage and output current. Maximum current concentration occurs when input voltage is in phase with output current. Table II describes current distribution of MC according to operating condition. It can be seen that at dc output condition, maximum current concentration occurs on conducting IGBTs. Dc output condition has higher current concentration ratio of 314% than normal ac output condition.

TABLE II. CURRENT DISTRIBUTION ACCORDING TO OPERATING CONDITIONS

Output frequency	Conducting devices per phase	Maximum current concentration on IGBT	Remarks
$f_{out} = 0$	3 IGBTs 3 diodes	314 %	Current concentration occurs on particular IGBTs but less severe than VSI because MC selects different IGBTs according to input voltage changes
$f_{out} \neq 0$ $f_{out} \neq f_{in}$	6 IGBTs 6 diodes	100 %	No current concentration occurs on particular IGBTs
$f_{out} = f_{in}$	6 IGBTs 6 diodes	225%	Conducting IGBTs become synchronized with output current. When output current is in phase with input voltage, maximum IGBT current concentration occurs

V. CONCLUSIONS

This paper has proposed an analytical method for evaluating power losses of bi-directional switches that consist of IGBT and diode in Matrix converter. Total losses consist of switching and conduction losses of IGBTs and diodes. Mathematical descriptions for calculating each loss component are presented. Current distribution of IGBTs according to output frequency is also investigated. 600V, 75A bi-directional switch modules are developed by integrating power IGBTs and diodes into one package. 200V, 7.5kW experimental setup is built using these modules, and total losses are measured at different carrier frequencies. The validity of the proposed analysis has been verified through comparisons between the calculated data and the experimental results.

REFERENCES

- [1] M. Venturini, "A new sine wave in sine wave out conversion technique which eliminates reactive elements," in Proc. Powercon 7, 1980, pp. E3-1-E3-15.
- [2] L. Huber and D. Borjovic, "Space vector modulated three-phase to three-phase matrix converter with input power factor correction," IEEE Trans. Ind. Applicat., vol. IA-31, No.6, pp.1234-1246, Nov. 1995.

- [3] J. Oyama, X. Xia, T. Higuchi, and E. Yamada, "Displacement angle control for matrix converter," in *Proc. IEEE PESC'97*, 1997, pp.1033-1039.
- [4] M. Hornkamp, M. Loddenkotter, and M. Munzer, O. Simon, M. Bruckmann, "Economac the first all-in-one IGBT module for matrix converters," *PCIM 2001*, Nurnberg, Germany, 2001, pp. 417-422.
- [5] M. Takei, Y. Harada, and K. Ueno, "600V-IGBT with reverse blocking capability," *ISPSD 2001*, Osaka, Japan, 2001, pp. 413-416.
- [6] S. Ishii, E. Yamamoto, H. Hara, E. Watanabe, A. M. Hava, and X. Xia, "A vector controlled high performance matrix converter – induction motor drive," in *Proc. IPEC-Tokyo2000*, 2000, pp.235-240.
- [7] J.K. Kang, H. Hara, E. Yamamoto, E. Watanabe, A.M. Hava, and T.J. Kume, "The matrix converter drive performance under abnormal input voltage conditions," *IEEE 32nd Annual Power Electronics Specialists Conference, PESC 2001*, Vancouver, Canada, June 2001, pp. 1089-1095.

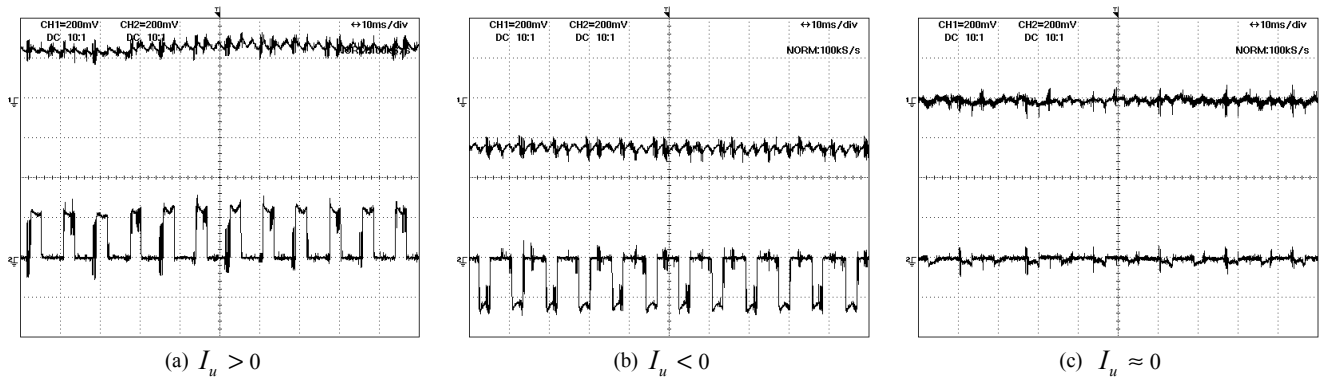


Fig.8. Current distribution in IGBTs of MC at 0Hz output frequency
U-phase output current (Upper trace) and I_{RU} (Lower trace)

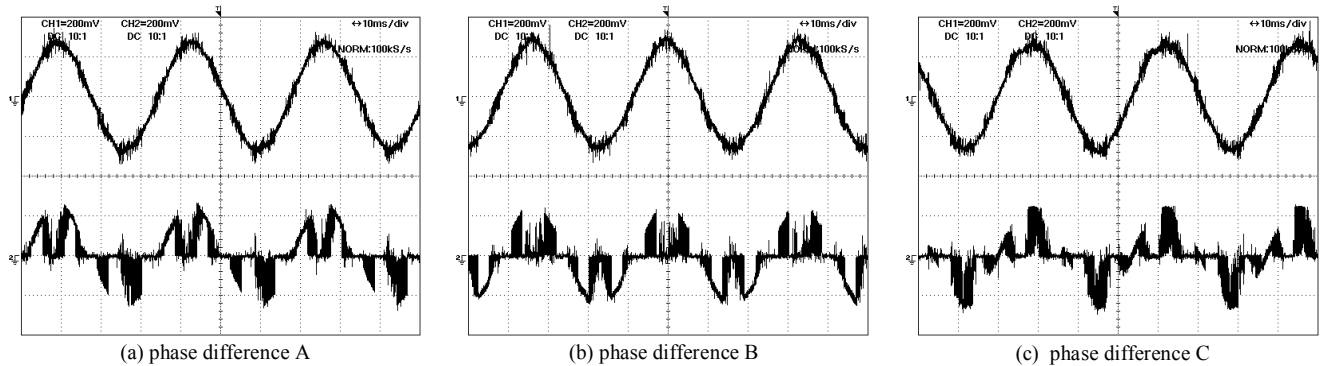


Fig.9. Current distribution in IGBTs of MC at 30Hz output frequency with three different phase differences between input voltage and output current.
U-phase output current (Upper trace) and I_{RU} (Lower trace)

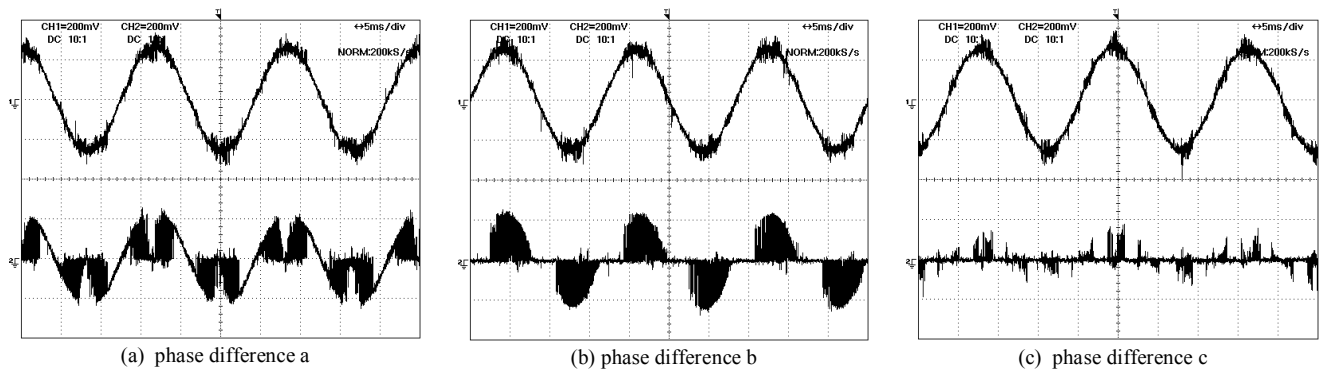


Fig.10. Current distribution in IGBTs of MC at 60Hz output frequency with three different phase differences between input voltage and output current.
U-phase output current (Upper trace) and I_{RU} (Lower trace)